8 System Throughput

8.1 Imaging Mode

Method:

Obtained images of the globular cluster M71 (NGC 6838) for which Clem, VandenBerg, and Stetson (2008) have high-precision photometry in the SDSS ugriz system (Fukugita et al. 1996 and Smith et al. 2002; we will drop the distinction between primed and unprimed, e.g., r' vs r, when referring to the SDSS bands). Data were acquired on the night of UTC 2010 Nov 18 during photometric conditions of a field centered at α=19:53:25.45, δ=+18:55:48.0 (J2000). Data were taken at around airmass 1.17. Table 26 lists the observations.

Table 30: M71 Photometric Calibration Field Images

Filter	Exp (s)	Airmass	FITS File
SDSS u	60	1.16	mods1b.20101118.0029.fits
	60	1.17	mods1b.20101118.0030.fits
SDSS g	10	1.14	mods1b.20101118.0024.fits
	30	1.15	mods1b.20101118.0025.fits
	30	1.15	mods1b.20101118.0026.fits
	10	1.15	mods1b.20101118.0027.fits
	10	1.16	mods1b.20101118.0028.fits
SDSS r	10	1.14	mods1r.20101118.0024.fits
	30	1.15	mods1r.20101118.0025.fits
	30	1.15	mods1r.20101118.0026.fits
	10	1.15	mods1r.20101118.0027.fits
	10	1.16	mods1r.20101118.0028.fits
SDSS i	30	1.16	mods1r.20101118.0029.fits
	30	1.16	mods1r.20101118.0030.fits
SDSS z	30	1.17	mods1r.20101118.0031.fits
	30	1.17	mods1r.20101118.0032.fits

Analysis:

Images in Table 26 were reduced (bias and sky flat), and then co-added to produce reference ugriz images for subsequent analysis. Aperture photometry was extracted using SExtractor (Bertin & Arnouts 1996). A world coordinate system was put onto the images using WCSTools, and the SExtractor catalog cross-correlated with the Clem et al. photometric catalog downloaded from the Strasbourg VizieR Catalogue Server (vizier.u-strasgb.fr).

Stars are chosen to be relatively unblended and not be saturated in any pixels. Between 40 and 56 suitable stars are measured in the griz images, and about 20 suitable stars in u band. Figure 55 shows the SDSS r image with the photometric calibration stars labeled.

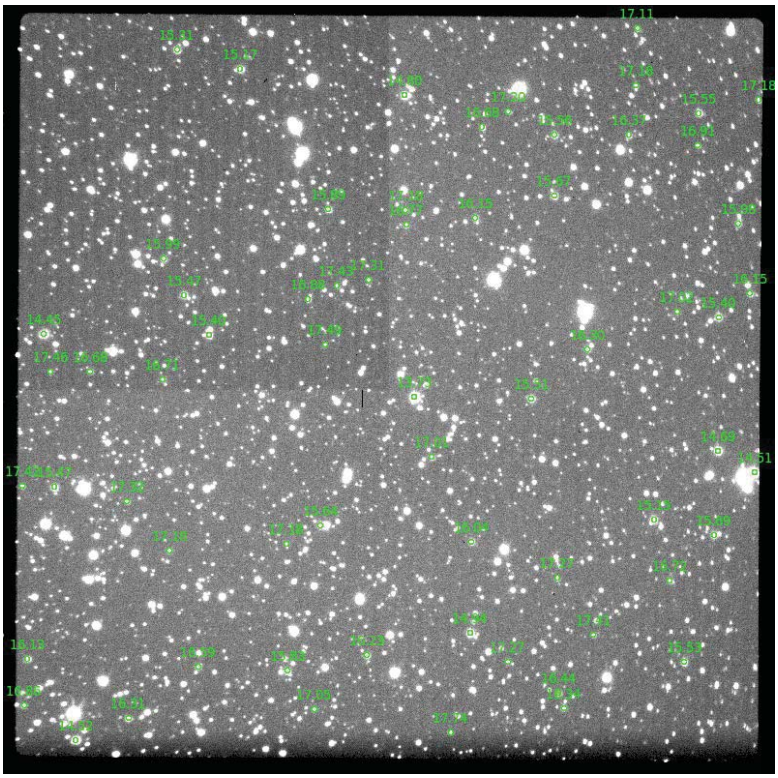

Figure 60: SDSS r image of the M71 photometric calibration field. Measured stars are shown in green with the r magnitudes.

Analysis of the photometry assumed atmospheric extinction coefficients for the site based on a combination of the measured LBC extinction coefficients, and our model LBT site extinction curve constructed by combining the well-measured KPNO and Cerro Paranal mean atmospheric extinction curves scaled to the LBT elevation of 3220 meters assuming an atmospheric scale height of 7 km.

Results:

Table 27 summarizes the zero-color photometric zero point magnitudes ($m_{f,0}$) for each filter measured from the M71 fields, corrected to outside the atmosphere using the estimated extinction coefficients (K_f).

Table 31: ugriz Photometry Zero Point Magnitudes

Filter	Nstars	$m_{f,0}$ (mag)	K_f
SDSS u	19	25.68±0.12	-0.47
SDSS g	48	27.38±0.03	-0.17
SDSS r	56	27.24±0.03	-0.10
SDSS i	44	27.21±0.04	-0.05
SDSS z	40	26.41±0.04	-0.03

The photometric conversion formula is

$$m_f = m_{f,0} - 2.5\log S_f + 2.5\log t_{\exp} + K_f X$$

where:

m_f = SDSS magnitude in filter f in AB units
S_f = Measured total counts in ADU in exposure time t_{exp} seconds
K_f = extinction coefficient for filter f
X = airmass at the time of the observation

An alternative way of expressing the zero points are in terms of predicted counts in ADU following the formula

$$\log S_f = \log S_{f,0} - 0.4 m_f + \log t_{\exp} - 0.4 K_f X$$

where:

log S_f = log counts in ADU for filter f
m_f = SDSS magnitude in filter f in AB units
t_{exp} = exposure time in seconds
log $S_{f,0}$ = ADU zero point (counts for m_f=0.0^{mag} in 1 second)
K_f = extinction coefficient for filter f
X = airmass at the time of the observation

Table 28 lists the ADU zero points (log $S_{f,0}$) for the five imaging filter bands.

Table 32: ugriz Photometry ADU Zero Points

Filter	log $S_{f,0}$
SDSS u	10.25
SDSS g	10.94
SDSS r	10.90
SDSS i	10.91
SDSS z	10.58

Taking account of pixel sampling and the typical PSF shape, the results of this table suggest that an r=15^{mag} star will just saturate the red CCD in 30sec in 0.6-arcsec seeing.

Using standard definitions of the SDSS bandpasses and the AB magnitude system, and adopting estimates of the reflectivity of the LBT SX Primary and Rigid Secondary in November 2010, we can convert the measured zero points into an estimate of the total throughput in imaging mode in the ugriz filter bands. We then compare the measurements to our model predictions based on the as-delivered coatings, and individual optical and detector efficiency estimates. The results are summarized in Table 29.

Table 33: Measured and Predicted Imaging Mode Efficiency

Filter	Predicted	Measured	Difference
SDSS u	20%	19%	-6%
SDSS g	52%	48%	-8%
SDSS r	67%	63%	-6%
SDSS i	68%	64%	-7%
SDSS z	43%	40%	-8%

It is notable that the difference (measured-predicted) is systematically about 7% on average. This is gray enough that the cause must be common to the red and blue channels. As will be seen in §8.2.1, the likely culprit is slightly lower than expected dichroic efficiency.

Color Terms

There is significant overlap between the stars measured on the griz images that we should be able to estimate first-order color terms in the transformation between MODS and SDSS magnitudes. However, the range of colors in these fields is too small (0.5 mag) to give much leverage. A basic examination finds no significant color terms larger than about 0.01 mag/color interval. This is expected as the MODS SDSS filters are very close to the design-reference bandpasses for the SDSS filters, and the combination of detector and atmosphere is not significantly different.

The lack of sufficient photometric weather during the times when we could go on-sky during commissioning means that we have limited spectrophotometric data to work with to derive more precise color terms, or to attempt independent estimation of atmospheric extinction coefficients (although the combination of LBC and spectral extinction coefficients described above is sufficient for our purposes).

8.2 Spectroscopic Mode

Method:

We obtained spectra of spectrophotometric standard stars derived from the HST CALSPEC database. These stars are a combination of the well-observed northern-hemisphere standards from the Oke list (1990 AJ, 99, 1621), and the four *Hubble Space Telescope* White Dwarf Primary spectrophotometric standards of Bohlin, Colina, & Finlay (1995 AJ, 100, 1316) (listed in boldface in Table 30).

Table 34: MODS Primary Spectrophotometric Standard Stars

Star	RA	Dec	Sp Type	m_{5556}	pmRA	pmDec
G191-B2B	05:05:30.613	+52:49:51.96	DA0	11.85	+7.45	–89.54
GD 71	05:52:27.614	+15:53:13.75	DA1	13.03	+85	–174
Feige 34	10:39:36.740	+43:06:09.26	sdO	11.25	+14.1	–25.0
Feige 66	12:37:23.517	+25:03:59.88	sdO	10.54	+3.0	–26.0
Feige 67	12:41:51.791	+17:31:19.76	sdO	11.89	–6.2	–36.3
GD 153	12:57:02.337	+22:01:52:68	DA1	13.35	–46	–204
Hz 43	13:16:21.853	+29:05:55.38	DA1	12.91	–157.96	–110.23
Hz 44	13:23:35.258	+36:07:59.51	sdO	11.74	–61.6	–3.1
BD+33°2642	15:51:59.886	+32:56:54.33	B2IV	10.81	–13.6	+0.7
BD+28 4211	21:51:11.021	+28:51:50.36	sdOp	10.56	–35.6	–58.7
Feige 110	23:19:58.398	–05:09:56.16	sdO	11.88	–10.7	+0.3
units	J2000	J2000		mag	mas/yr	mas/yr

For each primary standard star we created flux tables with 10Å sampling. These tables are in IRAF-style ASCII 3-column format ready to be used with IRAF or other programs, and available from the MODS website. Where necessary, we used HST stellar models or other HST calibration data to extend the near-IR coverage out to 10500Å, a little beyond the effective red limit of MODS around 10000Å. These are suitable for grating-mode calibrations. We also created 50Å-sampling flux tables suitable for prism-mode calibrations based on the Spec50 flux tables (Massey et al. 1988 ApJ, 328, 315) with the Massey & Gronwall (1990 ApJ, 358, 344). 50Å tables are not available for all primary standards.

For the flux star tables we censored all of the major telluric absorption complexes and the strongest stellar absorption lines. **Figure 56** graphically summarizes the primary standard stars for MODS. All of these stars are roughly the same color except the redder BD+33°2642, and span about 3 magnitudes in apparent brightness.

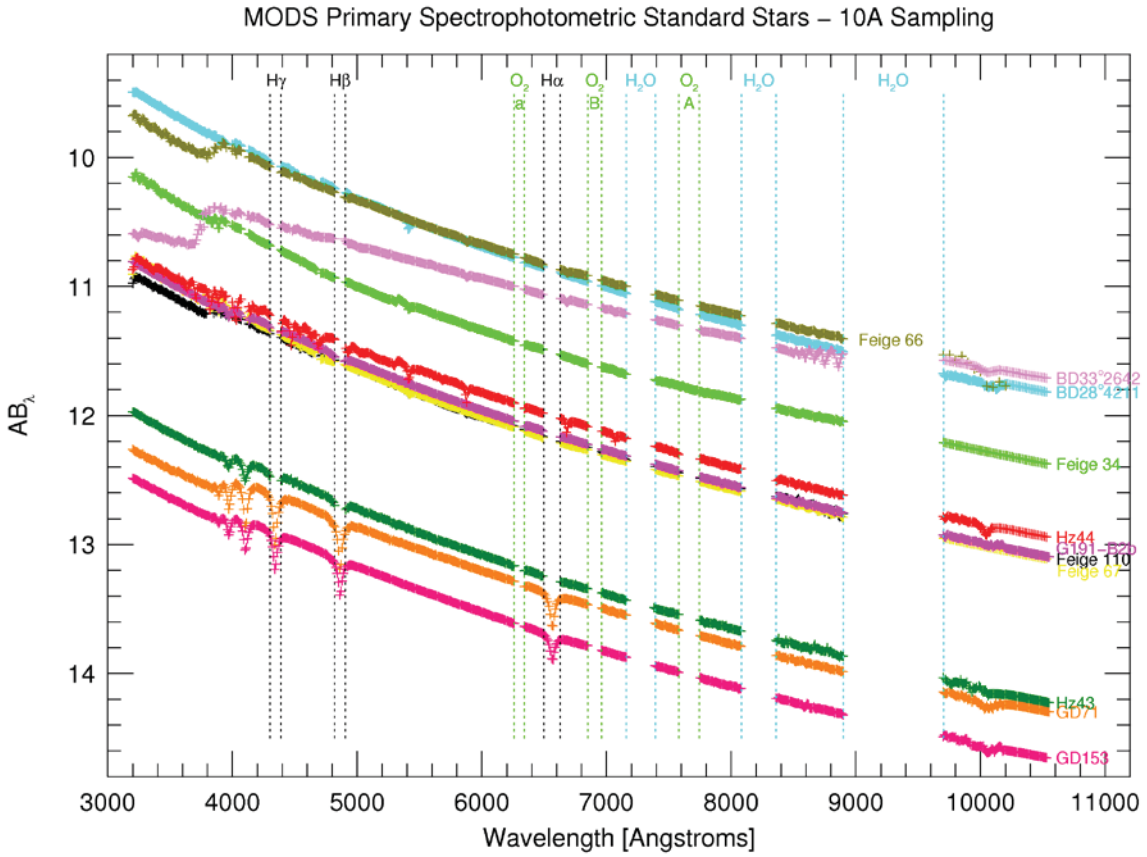

Figure 61: MODS Primary Spectrophotometric Standard Stars. Data are shown sampled in 10Å intervals plotted as AB magnitudes versus wavelength. The properties of the stars are summarized in Table 30.

Observations are obtained with the 5-arcsec wide spectrophotometric slit mask (LS60x5) to eliminate slit losses and loss of light due to differential atmospheric refraction at blue wavelengths (reduction in resolution is not an issue since we are averaging over 10Å bins). Exposure times are roughly comparable in both channels. Data were taken in the primary grating and prism modes, with and without the dichroic, for a total of 6 observations per standard star.

That was the plan, anyway. There was precious little photometric weather during the MODS1 primary commissioning runs, and the observations could not be obtained until we had (1) solved the lack of primary mirror baffling (see Appendix B), and (2) the wide spectrophotometric slit was cut (the mask was delivered before the March 2011 run), and (3) the WFS convergence issues were solved and we could make consistent images without "tails" (not solved until end of the March 2011 run). This meant that our first attempts at measuring spectroscopic efficiency did not begin until April 2011, and there was precious little photometric weather...

As such, we have had to troll through the data taken during the first shared-risk science runs in late 2011 through 2012 to find spectroscopic nights when OSU/RC observers were working (since in general until later in the science observing season for 2011/12 only OSU/RC observers were running the recommended flux calibration program with the recommended standard stars). Also, while observers often claimed it was "photometric" on the basis of the lack of clouds at sunset, this was rarely confirmed, so we had to troll through a *lot* of data to find suitable spectral standard star observations. There wasn't a lot of photometric weather during 2011/12 science operations time, either (at least not on OSU/RC nights).

This means our analysis will be limited to observations of a small number of stars taken under photometric conditions following the recommended observing protocols for MODS calibration with standard stars. We did not have an opportunity to take data at a wide range of airmasses to estimate the local extinction, so we must adopt an estimated extinction curve for the LBT site as described in §8.1.

For the analysis below, we used a set of spectra in all modes taken of the HST Primary White Dwarf Standard star GD71 on UTC 2011 Dec 25 under photometric conditions. The observers accidentally ran the full template scripts for all modes instead of editing it for just the dual-channel grating mode being used that run, a mistake they corrected during the remainder of the night and run. As a result we got an unexpected Christmas present. We have one other set of data of Feige 67, but only in dual-grating and red-only grating mode that corroborates the GD71 results. We therefore adopt the 2011 Dec 25 data set as our reference for computing the grating- and prism-mode efficiencies in the 6 spectral modes. The raw image files are listed in Table 31.

Table 35: GD71 Spectrophotometric Observations

Disperser	Mode	Exp (s)	Airmass	FITS File
Grating	Dual	180	1.04	mods1b.20111225.0028-30
				mods1r.20111225.0043-45
	Blue-Only	180	1.05	mods1b.20111225.0031-33
	Red-Only	180	1.05	mods1r.20111225.0046-48
Prism	Dual	30	1.06	mods1b.20111225.0034-36
				mods1r.20111225.0049-51
	Blue-Only	30	1.07	mods1b.20111225.0037-39
	Red-Only	30	1.06	mods1r.20111225.0052-54

All of the observations in Table 31 were made with the LS5x60 spectrophotometric calibration "fat slit" under apparently photometric conditions. The object was observed over the course of 1 hour between UTC 06:45 and 07:45.

8.2.1 Grating Spectroscopic Efficiency

For the grating modes, we used standard MODS and IRAF procedures to extract 1D spectra on a linear wavelength scale interpolated to a uniform 0.5Å pix^{-1} in units of ADU. These were processed using the IRAF NOAO onedspec tasks `standard` and `sensfunc` to derive sensitivity (aka "response") functions. These were converted into spectroscopic efficiency (instrument+telescope) as a function of wavelength using standard methods.

The resulting efficiencies for the grating spectroscopy modes are shown in Figure 57:

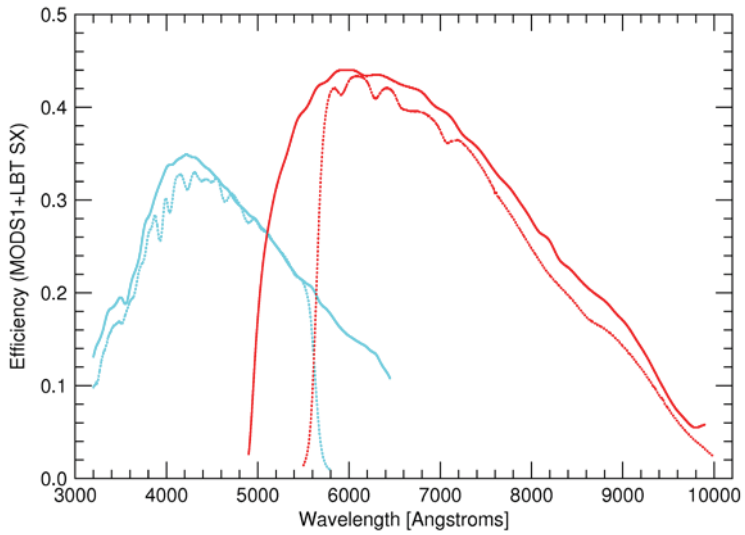

Figure 62: MODS1+LBT SX efficiencies in grating spectroscopy modes. Solid lines show direct (blue- and red-only) efficiencies, dashed lines are for dual (dichroic) modes.

These grating efficiency results are for MODS1 plus the LBT SX primary and secondary mirrors, exclusive of the atmosphere. Data were taken with the rigid and adaptive (AO2) secondary mirrors, and show no significant differences.

For planning purposes, the efficiencies above can be used to estimate counts (ADU) per wavelength interval in a given exposure time following the formula:

$$\log S_\lambda = \log S_{\lambda,0} + \log F_\lambda + \log t_{\exp} - 0.4 K_\lambda X$$

where:

$\log S_\lambda$ = log counts in ADU Å^{-1} at wavelength λ
$\log S_{\lambda,0}$ = Spectroscopic zero point in ADU Å^{-1} at wavelength , see Table 36
F_λ = flux in units of erg/sec/cm^2/Å
t_{exp} = exposure time in seconds
K_λ = Atmospheric Extinction Coefficient at wavelength λ
X = airmass at the time of the observation

A subset of the spectroscopic zero points as a function of wavelength for the MODS1 grating modes are summarized in Table 36.

Table 36: MODS1 Grating Mode Spectroscopic Zero Points

Red Grating			Blue Grating		
	log $S_{\lambda,0}$			log $S_{\lambda,0}$	
λ (Å)	Direct	Dichroic	λ (Å)	Direct	Dichroic
5000	15.978	...	3200	15.545	15.597
5500	16.381	14.922	3500	15.758	15.865
6000	16.465	16.453	4000	16.050	16.179
6500	16.487	16.473	4500	16.093	16.257
7000	16.488	16.462	5000	16.063	16.237
7500	16.456	16.433	5500	15.991	16.162
8000	16.391	16.341	5800	15.933	14.811
8500	16.310	16.242	6000	15.887	...
9000	16.229	16.151	6450	15.764	...
9500	15.963	15.893			
10000	15.802	15.396			

For a given source flux (F_λ) and exposure time, these coefficients allow a 10-20% prediction of the approximate ADU in the seeing disk by multiplying the predicted spectral counts S_λ by the nominal spectral pixel size in Å (~0. 85Å pix^{-1} in red and 0.50Å pix^{-1} in blue; §7.2.1). The effect of atmospheric extinction is factored in by selecting a nominal airmass for the observation and applying an appropriate model for the atmospheric extinction. The coefficients given in the adopted model LBT extinction curve do not include strong telluric absorption features, so this correction should be done with some caution if using it to predict signal in a given exposure time at wavelengths in proximity to strong telluric features.

These sensitivity estimates do not include slit losses, which depend on seeing and other factors not easily quantified, and do not factor in changes in telescope reflectivity as mirrors get dirty or are cleaned, cirrus, etc., so are meant to provide basic (10-20%) guidance in observing planning.

8.2.2 Prism Spectroscopic Efficiency

This mode has been less utilized in practice, especially in the blue- and red-only modes, so we have even less photometric standard star data for prism mode than grating. Nonetheless, we were able to measure the prism mode efficiency using archival data.

Because of the strong wavelength-dependence of dispersion in the prisms (see §7.2.2), we followed a different procedure. After extracting 1D spectra, we applied a wavelength calibration on a polynomial rather than linear scale to preserve the raw pixels, and then computed sensitivity functions using the 50Å sampled flux tables using custom Python scripts. These were then converted into efficiency curves from the sensitivity functions.

The resulting efficiencies for the prism spectroscopy modes are shown in Figure 58.

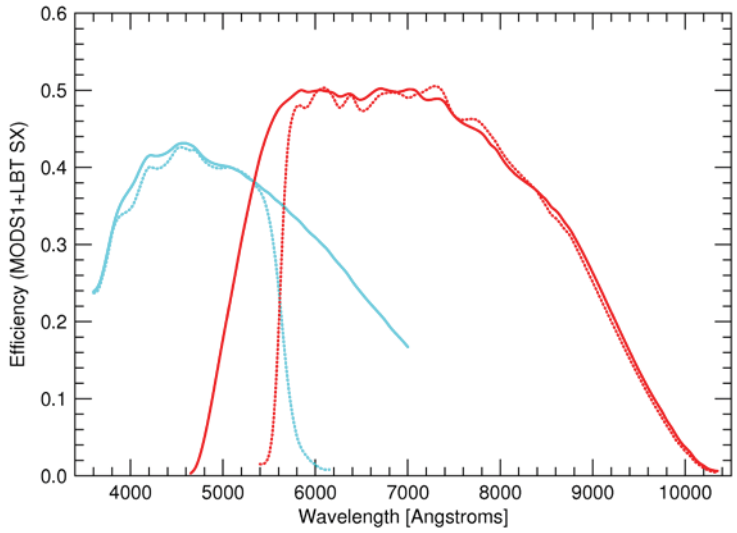

Figure 63: MODS1+LBT SX efficiencies in prism spectroscopy modes. Solid lines show direct (blue- and red-only) efficiencies, dashed lines are for dual (dichroic) modes.

A subset of the spectroscopic zero points as a function of wavelength for the MODS1 grating modes are summarized in Table 37.

Table 37: MODS1 Prism Mode Spectroscopic Zero Points

Red Prism				Blue Prism			
	log $S_{\lambda,0}$		Pixel		log $S_{\lambda,0}$		Pixel
λ (Å)	Direct	Dichroic	δλ (Å)	λ (Å)	Direct	Dichroic	δλ (Å)
5000	15.722	...	2.6	3600	15.663	156.640	3.4
5500	16.178	14.978	3.4	3850	15.886	15.858	4.4
6000	16.268	16.265	4.6	4030	15.978	15.927	5.1
6450	16.301	16.293	5.9	4500	16.121	16.096	7.1
7000	16.357	16.348	7.6	5000	16.162	16.138	9.8
7450	16.365	16.368	9.1	5500	16.172	16.112	12.7
8000	16.342	16.350	11.2	6000	16.143	15.478	15.8
8500	16.307	16.297	13.3	6450	16.082	...	18.5
8800	16.264	16.252	14.6	7000	15.964	...	21.8
9750	15.740	15.692	18.9				
10000	15.396	15.333	20.1				

Some of the wavelengths in Table 37 are chosen to avoid strong telluric or stellar absorption features in the standard stars spectra, and so are intentionally not on a regular grid. For the prism spectra we obtained the detailed flux calibration did not extend below 3600Å because of a lack of a good wavelength solution below 3500Å. The same formula for estimating counts per exposure time used for the grating mode apply to data in this table for the prism, but bear in mind that the size of spectral pixel is a strongly varying function of wavelength. Nominal pixel sizes are given in the final column for each side in Table 37 (see also §7.2.2, specifically Figure 51 and Figure 57).